CTD OXYGEN SENSOR CALIBRATION PROCEDURES

H. Uchida[1], G.C. Johnson[2], and K.E. McTaggart[2]

[1] Research Institute for Global Change, Japan Agency for Marine–Earth Science and Technology, 2-15 Natsushima, Yokosuka, Kanagawa 237-0061, Japan, e-mail: huchida@jamstec.go.jp.

[2] NOAA/Pacific Marine Environmental Laboratory, 7600 Sand Point Way NE Bldg. 3, Seattle WA 981115, U.S.A, e-mail: gregory.c.johnson@noaa.gov, kristene.e.mctaggart@noaa.gov.

1.   INTRODUCTION

Oxygen sensors currently afford one of the few opportunities to acquire accurate measurements of a biogeochemical parameter at the same vertical resolution as CTD data.   Electrochemical cells have been used to measure dissolved oxygen concentration in a water solution, initially blood (Clark et al., 1953) but soon thereafter aquatic environments (Kanwisher, 1959) for many decades.   More recently, optical sensors have been applied to aquatic uses (Klimant et al., 1995).   Here we present outlines of procedures on acquisition, processing, and calibration of oxygen data collected from both electrochemical and optical oxygen sensors.   We focus only on one model of electrochemical cell, specifically the SeaBird Electronics SBE-43.   Here also we provide detailed material on recent experience with acquisition, processing, and calibration of data from optical oxygen sensors, specifically the Aanderaa Data Instruments Optode 3830 and the JFE Alec Rinko Optode.   For all sensor types, readers should bear in mind that oceanic oxygen measurement and calibration techniques are subject to improvement.   This outline should be viewed only as a supplement to the existing literature, manufacturer documentation, and manufacturer instructions.

2.   ELECTROCHEMICAL SENSORS

2.1   Maintenance, Storage, Transport, Assembly, and Monitoring

Sea-Bird Electronics SBE-43 electrochemical oxygen sensors, when used for high-quality repeat hydrographic sections, should always be recalibrated prior to each expedition or, if needed, refurbished (electrolyte refilled, membrane replaced, and recalibrated).   Taking at least three sensors on each cruise, but deploying only one at any given time, allows for spares should any sensor fail. The manufacturer provides extensive and thorough recommendations for transport and storage of the SBE-43 oxygen sensors, their plumbing when assembling the CTD and sensors, and their routine care at sea.   We do not repeat these instructions here.   However, we do note that following these recommendations generally results in collection of good data that can be calibrated to a high accuracy using in situ bottle oxygen data from water sample titrations.   However, oxygen sensors do sometimes fail, so it is important to assess their performance continually during a cruise.

The health of the sensor can be assessed during the cruise in several ways.   First, a visual assessment of the oxygen profile should be made during each station, watching for sudden shifts, spikes, or other suspicious features in oxygen data.   Second, the time-history of the oxygen data profiles should be monitored during the cruise, comparing one profile to the next to check for unexpected profile-to-profile shifts in observed values.   Third, attempts should be made to calibrate the oxygen profile data to in situ bottle oxygen data from water sample titrations throughout the cruise.   If

large changes in calibration parameters are necessary to fit the sensor data from subsequent stations accurately to the bottle data, there may be problems. Finally, the calibrated data should be compared to historical data in the region, if they are available and as time allows. If the performance of the oxygen sensor is in serious doubt (for instance, seeing either noisy oxygen data or oxygen values falling rapidly and unexpectedly from profile to profile may cast doubt on oxygen sensor performance) the old sensor should be replaced between stations. However, operators should bear in mind that pump malfunctions and electrical problems can also cause problems in oxygen data.

2.2   Sensor Data Acquisition and Processing

Oxygen sensor voltage (0-5 V) from the SBE-43 can be acquired by integrating the sensor into a SBE-9plus CTD and routing the signal through a SBE-11plus V2 Deck unit to a computer running Seasave V7 software. Data acquisition and processing are described in detail in documentation from the manufacturer, as outlined in the companion chapter on CTD data acquisition, processing, and calibration. However, a few issues unique to the oxygen sensors are discussed here.

First, electrochemical oxygen sensors generally exhibit a sensor response time τ of several seconds. This response time describes how long it takes a sensor to equilibrate with its surroundings as oxygen diffuses across its membrane. SeaBird suggests modeling as the following function of temperature and pressure:

$$\tau = \tau_{20} \cdot \exp(D_1 \cdot p + D_2 \cdot (T - 20)) \qquad (1)$$

where τ is the oxygen sensor response time, τ_{20} is the response time at 20°C and atmospheric pressure, p is the measured pressure, and T is the temperature. SBE will provide the three coefficients, τ_{20}, D_1, and D_2 for each oxygen sensor as part of their laboratory calibrations. These coefficients can be used with SBE data conversion software to estimate the sensor response time and thus compensate for oxygen lags. SBE suggests correcting the lag using oxygen rate of change estimated using a default 2-second window in their data conversion software. However, if oxygen data are noisy, using a slightly longer window (up to 5 seconds) to estimate the time derivative may help to reduce noise generated by the lag correction. Alternatively, one can attempt to fit a subset of these coefficients (perhaps only τ_{20}) during the water-sample field calibration process, and apply a sensor response time correction to the oxygen data at that time.

Second, electrochemical oxygen sensors that experience the high pressures of full depth sampling (in practice p > 1000 dbar) exhibit a noticeable hysteresis, with oxygen sensor voltages during descent sometimes considerably higher than voltages at the same pressures during ascent. The magnitude of the hysteresis is dependent on the entire pressure-time history of the sensor during a typical CTD station, apparently because of a several-hour memory of the sensor membrane to pressure forces (Edwards et al., 2010).

Because CTD intakes are generally located to minimize wake interference as the CTD is descending, down-cast profile data are generally reported from CTD profiles. The up-cast data are primarily sub-sampled during times of bottle closing (a typical sub-sample might be an 8-second average centered on the bottle closing). CTD pressure, temperature, and conductivity sensor data from the up-cast subsamples can be used together with salinity measurements made from water samples using

an autosalinometer to produce a calibrated CTD salinity profile from the downcast data. However, oxygen sensor hysteresis complicates the calibration of down-cast (descending) oxygen profiles with oxygen measurements from water samples collected by closing Niskin bottles during the up-cast (ascent). There are two methods of correction for this effect.

First, SBE has recently developed a sensor response correction equation for the hysteresis and will provide sensor response coefficients for this hysteresis with oxygen sensor calibrations. These coefficients can again be used with SBE data conversion software to compensate for oxygen sensor hysteresis. In theory, this correction should allow calibration of down-cast CTD oxygen profiles by using CTD oxygen data collected on the up-cast at the times of water sample collection to calibrate the down-cast oxygen data. The authors have not yet thoroughly applied this method to a repeat hydrographic section data set.

Another method is simply to match the down-cast profile data to the up-cast water sample data by pressure or an appropriate density parameter (either neutral density or appropriately referenced potential densities). Using this method, the pressure, temperature, salinity, and oxygen voltage values from the down-cast CTD/O_2 profile data can be calibrated to the oxygen concentrations from up-cast water samples. Pressure matching is self-explanatory but since water-properties follow isopycnals and those can heave substantially between up-cast and down cast, this procedure can introduce some noise into estimations of calibration coefficients. Matching by an appropriate density parameter is more suitable, but has some pitfalls. Neutral densities are applicable throughout the water column, but if potential densities are used, they should be appropriately referenced (match water samples collected between the surface and 1000 dbar to the CTD/O_2 down-cast profile data using potential density referenced to 500 dbar and so on down the water column). In low vertical density gradient regions (within the surface mixed layer and possibly within nearly vertically homogenous abyssal layers) one should revert to pressure matching.

2.3   Calibration Data

The methodology for collection, titration, standardization, and reporting of accurate oceanic dissolved oxygen concentration data from water samples collected during the CTD upcast is described in another chapter of this manual. Water sample oxygen data should be in μmol kg^{-1} when used to calibrate CTD oxygen profile data, to ensure that the profile is reported in those units.

2.4   Sensor Calibration

SBE does not presently provide software for determining calibration equation coefficients. One goal is to minimize the residual of the squared differences of calibrated oxygen data and the water sample data by adjusting coefficients for a physically motivated calibration equation. Another goal is to maximize the number of samples used to determine a set of coefficients, that is to use data from the largest number of consecutive stations possible to determine a fit. Oxygen sensor calibration equations are non-linear, so a non-linear fitting routine is usually required. In some cases there are expected limits for some coefficients (sensor lag times are expected to be positive and on the order of a few seconds, for instance), so constrained minimizations can be used.

Oxygen sensor calibration equations are usually refinements of or modifications to the form proposed by Owens and Millard (1985):

$$O_2 = S_{oc} \cdot \left(V + V_{off} + \tau \cdot dV/dt\right) \cdot O_{sat} \cdot e^{(T_{cor} \cdot (T + w_T \cdot (T_o - T)))} \cdot e^{(p_{cor} \cdot p)}, \qquad (2)$$

where O_2 is the CTD oxygen (in µmol/kg if the water sample data used are in those units), V is oxygen voltage, dV/dt is the temporal gradient of the oxygen voltage (in volts/s estimated by running linear fits made over 2 seconds nominally, but possibly longer), t is time, T is CTD temperature, T_o is oxygen sensor temperature, p is CTD pressure, and O_{sat} is oxygen saturation (a function of salinity, temperature, and pressure; e.g. García and Gordon, 1992). In this equation S_{oc}, V_{off}, τ, W_T, and p_{cor} are all calibration equation coefficients that are estimated by a non-linear least squares fit to oxygen water sample data.

Seabird currently suggests the following calibration equation for the SBE-43:

$$O_2 = S_{oc} \cdot \left(V + V_{off} + \tau_{20} \cdot e^{(D_1 \cdot p + D_2 \cdot (T - 20))} \cdot dV/dt\right)$$
$$\cdot O_{sat} \cdot (1 + A \cdot T + B \cdot T^2 + C \cdot T^3) \cdot e^{[(E \cdot p)/(273.15 + T)]} \qquad (3)$$

which takes a form slightly different from the first equation. First, the sensor lag is pressure and temperature dependent, being τ_{20} at atmospheric pressure and 20°C, but longer for colder temperatures and higher pressures, a modification with physical basis (Edwards et al., 2010). Second, much of the temperature correction for the sensor is done in the electronics, and oxygen temperature is not reported by the SBE-43, so T_o does not appear in the temperature correction terms. Instead of an exponential, the suggested temperature correction is a 3rd order polynomial. Third, the last term, mostly a pressure correction, is also a function of absolute temperature (a relatively small effect for oceanographic temperature ranges, but physically motivated, e.g. Atkinson et al., 1996).

SBE provides the calibration coefficients S_{oc}, V_{off}, τ_{20}, D_1, D_2, A, B, C, and E with their oxygen sensor calibrations. However, in practice, some subset of these coefficients should be determined by non-linear least squares fits to in situ water sample oxygen data. Certainly S_{oc} and perhaps V_{off} should be expected to vary for each sensor over the course of its use during a cruise. In practice, groups still use different variants of oxygen sensor calibration equations.

For instance, the ODF group at UCSD/SIO uses an equation of the form

$$O_2 = [C_1 \cdot V \cdot e^{(C_2 \cdot p_h/5000)} + C_3] \cdot O_{sat} \cdot e^{(C_4 T_l + C_5 T_s + C_6 p_l + C_7 dp/dt + C_8 dT)}, \qquad (4)$$

where $C_1 - C_8$ are fitted coefficients, p_h is a low-pass-filtered hysteresis pressure, T_l is a long-response low-pass filtered temperature, T_s is a short-response low-pass filtered temperature, p_l is a low-pass filtered pressure, and $dT = T_f - T_s$ is a low-pass filtered thermal diffusion estimate (e. g. Swift and Johnson, 2009). The coefficients for the lagged terms in the model are typically determined for each sensor and held fixed for an entire cruise, whereas at least the sensor slope (C_1) and offset (C_2) coefficients are usually allowed to vary as functions of station. Down cast oxygen sensor data are matched to up-cast water sample data in density coordinates, which helps mitigate the oxygen sensor hysteresis.

The CTD group at NOAA/PMEL has yet to use the SBE hysteresis correction for oxygen sensor calibrations during a cruise, and also still matches down-cast CTD oxygen data to up-cast water-

sample oxygen data by appropriately referenced potential densities. They use an oxygen sensor calibration equation of the form

$$O_2 = S_{oc} \cdot \left(V + V_{off} + \tau_{20} \cdot e^{(D_1 \cdot p + D_2 \cdot (T-20))} \cdot dV/dt \right) \cdot O_{sat} \cdot e^{[Tcor \cdot T]} \cdot e^{[(E \cdot p)/(273.15+T)]}, \quad (5)$$

where S_{oc}, V_{off}, τ_{20}, T_{cor}, and E are determined during the fit, with D_1 and D_2 fixed at values given in the SBE sensor calibration sheets for each sensor. At least without hysteresis correction, fitting an exponential temperature correction rather than using a third-order polynomial temperature correction (either with the coefficients provided by SBE or attempting to fit coefficients) can lead to smaller and more randomly distributed residuals between calibrated sensor and water sample oxygen data. The fit is first attempted using one set of equation coefficients for the entire data set, initializing the non-linear minimization with a set of expected values. By examining the residuals from that fit as a function of station number, the stations are broken into groups as deemed appropriate to minimize residuals as a function of station number, pressure, and temperature while limiting the number of groups used. New coefficients are determined for each group. A station-dependent S_{oc} value (a linear function of station number) is allowed in a group if warranted, while keeping all other coefficients constant for that group. All fits are iterative, discarding outliers exceeding 2.8 standard deviations of the fit residuals until no more outliers are discarded.

2.5   Discussion

Collecting and calibrating electrochemical oxygen sensor profiles of dissolved oceanic oxygen data requires some expertise and perhaps some art as well. When calibrations are complete, the residuals between oxygen sensor data and bottle oxygen sample data should be small (< 2 μmol kg^{-1} overall and even < 1 μmol kg^{-1} in some locations of the water column) if water sample data quality are high and oxygen sensor performance is good. Residuals should also be randomly distributed, with no obvious patterns when inspected as functions of station number, pressure, temperature, or oxygen concentration.

3.   OPTODES

3.1   Background

Oxygen optodes (also called optrodes) have been introduced to aquatic research (Klimant et al., 1995). Recently, an oxygen optode sensor (Oxygen Optode model 3830; Aanderaa Data Instruments AS, Bergen, Norway) became commercially available for aquatic research (Körtzinger et al., 2005; Tengberg et al., 2006). This optode's measurement principles have been described in detail (Demas et al., 1999).

Oxygen optodes are based on the oxygen luminescence quenching of a platinum porphyrin complex (fluorescent indicator) that is immobilized in a sensing foil. Optodes show a nonlinear decrease in luminescence decay time with increasing oxygen concentration. The signal can be linearized by means of the Stern–Volmer equation: $[O_2] = (\tau_0/\tau - 1)/K_{sv}$, where $[O_2]$ is oxygen concentration in μmol L^{-1}, τ is luminescence decay time, τ_0 is the decay time in the absence of $[O_2]$, and K_{sv} is the Stern–Volmer constant (Demas et al., 1999). The fluorescent indicator is excited with blue light with sinusoidally modulated intensity and emits a red luminescent light. The phase angle between the excited and emitted signals is shifted as a function of the ambient oxygen concentration. In a

5

lifetime-based measurement, phase-shift is detected instead of decay time. Although Aanderaa Data Instruments AS uses a fully empirical equation (a fourth-order polynomial in phase-shift data of an optode with coefficients of a third-order polynomial in temperature) for laboratory calibration (Uchida et al., 2008), the oxygen optodes can be calibrated accurately with the Stern–Volmer equation expressed in terms of phase-shift data:

$$[O_2] = (P_0/P_c - 1)/K_{sv}, \tag{6}$$

and

$$K_{sv} = c_0 + c_1 T + c_2 T^2, \; P_0 = c_3 + c_4 T, \text{ and } \quad P_c = c_5 + c_6 P_t, \tag{7}$$

where T is temperature in °C, P_t is the raw phase-shift data of the optode sensor in degrees, P_0 is the phase shift in the absence of $[O_2]$, and c_x ($x = 0, 1, ..., 6$) are the calibration coefficients (Uchida et al., 2008). The ratio of the decay time (τ_0/τ) used in the classical Stern–Volmer equation is replaced in equation (6) with the ratio of the phase shift (P_0/P_c). The relationships in the calibration equations can be confirmed by the results of the manufacturer's calibration (a 35-point calibration of five temperatures and seven oxygen concentrations; Aanderaa Data Instruments AS). Although the Stern–Volmer plots are never perfectly linear, they approach linearity (Fig. 1). The temperature dependence of the Stern–Volmer constants (K_{sv}) obtained from the data in Fig. 1 can be expressed as a second-order polynomial for each batch of sensing foil of the optode (Fig. 2). The oxygen optodes show a linear decrease in the phase-shift data with increasing temperature in the absence of $[O_2]$ (Fig. 3).

Because the sensing foil of the optode is permeable only to gas and not to water, the optode cannot sense the presence of salt dissolved in the water. Moreover, the response of the sensing foil decreases with increasing ambient pressure. Therefore, the temperature-compensated optode oxygen data must be corrected both for salinity and for pressure. For the Optode 3830, the pressure-compensated oxygen concentration ($[O_2]_c$) can be calculated from the following equation:

$$[O_2]_c = [O_2](1 + C_p p/1000), \tag{8}$$

where p is pressure in dbar, and C_p is the compensation coefficient. The best choice for the C_p value is estimated to be 0.032 by in situ calibration of the oxygen optodes (Uchida et al., 2008). The salinity-compensated oxygen concentration ($[O_2]_{sc}$) can be calculated by multiplying the factor of the effect of salt on the oxygen solubility (e.g. García and Gordon 1992):

$$[O_2]_{sc} = [O_2] \exp[S(B_0 + B_1 T_S + B_2 T_S^2 + B_3 T_S^3) + C_0 S^2], \tag{9}$$

where S is salinity, T_S is scaled temperature ($T_S = \ln[(298.15 - T)/(273.15 + T)]$), and B_x ($x = 0, 1, 2, 3$) and C_0 are solubility coefficients. García and Gordon (1992) recommend the use of the solubility coefficients derived from the data of Benson and Krause (1984; $B_0 = -6.24523e^{-3}$, $B_1 = -7.37614e^{-3}$, $B_2 = -1.03410e^{-2}$, $B_3 = -8.17083e^{-3}$, $C_0 = -4.88682e^{-7}$).

If the CTD profiler is not able to receive the digital (RS232) output from the Optode 3830, an analog adapter (model 3966; Aanderaa Data Instruments AS) must be used to convert the digital signals to analog signals in terms of voltage. The phase-shift data (P) in degrees can be calculated from the voltage: $P = 12 \times V + 10$, where V is voltage (0–5 V). In contrast, a prototype of another optode-

based oxygen sensor (Rinko; JFE Alec Co., Ltd., Kobe, Japan) has been developed, and the analog output (V) of this Rinko optode is directly used without conversion to the phase shift. Therefore, P_0, P_c, and P_r in equations (6) and (7) are replaced with V_0, V_c, and V_r, respectively, where V_r is the raw analog signal data in volts and V_0 is the analog signal in the absence of [O_2]. Furthermore, the response of the Rinko sensor's sensing foil to ambient pressure is not linear, and the pressure-compensated oxygen concentration can be calculated as $[O_2]_c = [O_2](1 + C_p p/1000)^{1/3}$. The C_p value for the Rinko prototype is estimated to be about 0.12 (0.058) for the optical window of acrylic (quartz) glass.

The oxygen concentration in volumetric units (μmol L^{-1}) can be converted to gravimetric units (μmol kg^{-1}) by dividing by water's potential density calculated from the CTD pressure, temperature, and conductivity (salinity) data.

3.2   Calibration Data

Calibration data are required to determine the coefficients of the algorithm shown in equations (6) and (7). In general, downcast profile of oxygen sensor data are used for analysis, although water samples are taken during the upcast. For in situ calibration, the oxygen data in the water samples measured by means of Winkler (Dickson 1996) or other appropriate titration methods (see manual chapter on oxygen titrations) are first merged with the appropriate oxygen sensor data to be calibrated. If the oxygen sensor is not flow-sensitive and the time-dependent, pressure-induced effect on the sensing foil does not exist, the oxygen sensor data at water sampling layers collected during the upcast profile can be used for in situ calibration.

The Optode 3830 data obtained during the bottle-firing stop for collection of a water sample can be used for in situ calibration, since the difference between the downcast and upcast oxygen profiles is relatively small (~1 μmol kg^{-1}; Uchida et al., 2008). The error in the Optode 3830 data caused by slow response time can be reduced if the water sample bottle is closed after allowing sufficient time for sensor equilibration after the stop. For example, the error is generally small (<1.5 μmol kg^{-1}) if the water sample bottle is closed 30 s after the stop (Uchida et al., 2008).

The data obtained from the Rinko optode during the bottle-firing stop can be assumed to be at equilibrium, since the Rinko optode has a fast time response (63% response time requires 0.7 s at a temperature of 26°C and 1.6 s at a temperature of 0°C). However, the time-dependent, pressure-induced effect on the sensing foil is large for the Rinko optode, as observed for a Clark electrode oxygen sensor (SBE 43; Sea-Bird Electronics, Inc., Bellevue, Washington). Although the difference (~3 μmol kg^{-1}) between the downcast and upcast profiles caused by the pressure hysteresis is slightly smaller for the Rinko optode than for the SBE 43 electrode (~5 μmol kg^{-1}), the hysteresis characteristics are similar between the two oxygen sensors so the hysteresis for the Rinko optode can be corrected by means of the same method as that developed for the SBE 43 electrode (Edwards et al., 2010). Therefore, the Rinko optode data can be calibrated by using the pressure hysteresis-corrected optode data at water sampling layers collected during the upcast profile (Murata et al., 2009). The calibration coefficients, H1 (amplitude of hysteresis correction), H2 (curvature function for hysteresis), and H3 (time constant for hysteresis) are typically 0.0065, 5000 dbar, and 2000 seconds, respectively, for the Rinko optode (The hysteresis algorithms are shown in Sea-Bird Electronics, Inc., 2009).

Although both the Optode 3830 and the Rinko optode have an internal temperature sensor, temperature compensation for calculation of the optode oxygen data should be performed using the high-quality CTD temperature data instead of the less accurate temperature data from the optodes' temperature sensors.

The calibration of optode oxygen data is weakly dependent on the calibration of CTD pressure, temperature, and conductivity (salinity) data. For example, a maximum error of 1% in optode oxygen data results from a pressure error of 250 dbar, or a temperature error of 0.2 °C, or a salinity error of 1 (1978 Practical Salinity Scale). Therefore, pressure, temperature, and conductivity (salinity) data should be calibrated prior to in situ calibration of optode oxygen data.

3.3   Determining Algorithm Coefficients

To calibrate an optode-based oxygen sensor with equations (6) and (7), a nonlinear parameter estimation technique is required to determine the best-fitting set of coefficients for the water sample observations. A method of minimizing the mean square deviation (least-squares regression) is often used. For least-squares regression, the data sometimes need to be edited to remove spurious points (Millard 1994). When there are outlier points to a Gaussian model for experimental error, the method of minimizing the mean absolute deviation is more robust than the method of minimizing the mean square deviation (Press et al., 1992). Some algorithms, including the quasi-Newton method, the Levenberg–Marquardt method, and the Nelder–Mead simplex search, are available for nonlinear parameter estimation (Press et al., 1992).

When all coefficients of equation (7) are estimated simultaneously, the coefficients of P_0 and P_c will strongly depend on initial values of the coefficients of P_0 and P_c, and cannot be determined uniquely. Therefore, P_0 and P_c are normalized by the phase shift in the absence of [O_2] at 0 °C. The ratio of the phase shift can be rewritten as:

$$P_0/P_c = (1 + d_0T)/(d_1 + d_2P_r), \tag{10}$$

where $d_0 = c_4/c_3$, $d_1 = c_5/c_3$, and $d_2 = c_6/c_3$. From this equation, six coefficients (c_0, c_1, c_2, d_0, d_1, and d_2) must be determined for the calibration.

Residuals between the optode oxygen data and the Winkler oxygen data have to be minimized. The residual can exhibit global (truly the lowest value) or local (the lowest in a finite neighborhood) minima. It is necessary to employ pre-set values for the six coefficients mentioned above in the nonlinear parameter estimation (e.g. Table 1). When attempting to fit a relatively small number of data points, the residual might not converge to a global minimum. To estimate the best-fitting set of coefficients, it may be helpful to fix coefficients for P_0 (i.e., c_3 and c_4) with suitable values, such as values estimated from laboratory experiments using a 0% oxygen solution at various temperatures. If the observed range of temperature is small, then K_{sv} may be approximated by a straight line. It is also useful to change the pre-set coefficients repeatedly and to fit them with weighting factors to determine the best-fitting set. The weight assigned to each coefficient may be expressed as a function of vertical oxygen gradient.

As an example, the Optode 3830 and Rinko optode are calibrated with Winkler oxygen data collected from water samples obtained in the Bering Sea and the northwest subarctic Pacific Ocean on the R/V *Mirai* cruise MR08-05 (Fig. 4). The calibration coefficients are determined by minimizing the

mean absolute deviation from the Winkler oxygen data by means of the revised quasi-Newton method (FORTRAN subroutine DMINF1 from the Scientific Subroutine Library II, Fujitsu Ltd., Kanagawa, Japan). The water sample bottles were closed 30 s after the stop to collect water samples, and the Optode 3830 and Rinko optode data obtained during the period when the bottle was closed are used for the calibration. For the Optode 3830, the coefficient d_1 is changed for each CTD station, since data from the Optode 3830 slightly fluctuated at every CTD station. The standard deviation (SD) of the estimated offset for the phase shift is about 0.05 degrees, corresponding to an oxygen concentration of 0.2–1 µmol kg^{-1}. This in situ calibration method provides sufficiently accurate calibration results, with a coefficient of variation (CV) of 0.36% for pressure ≥1000 dbar. For the Rinko optode, the values of all six coefficients except for d_0 are changed for each CTD station, since data from the Rinko optode shows a large time drift. This time drift primarily is caused by a change in the span slope (c_6 or d_2) rather than a change in the offset (c_5 or d_1) drift of the raw phase shift data of the Rinko optode. The span slope changes almost linearly by about 10% over 17 days. The Rinko optode could also be calibrated with sufficient uncertainty relative to the Winkler oxygen data, with a CV of 0.30% for pressure ≥1000 dbar.

Since the Rinko optode shows relatively large calibration drift with time, the following modification of the equation (10) is also effective:

$$P_0/P_c = (1 + d_0 T)/(d_1 + d_2 P_r + d_3 t + d_4 P_r t), \qquad (11)$$

where d_3 and d_4 are additional calibration coefficients, and t is time. The calibration coefficients could be estimated simultaneously with sufficient uncertainty for the Rinko optode data obtained on 109 stations over 23 days (Murata et al., 2009).

3.4   Discussion

A procedure for calibrating optode-based oxygen sensors is presented in this report. Oxygen data obtained from the Optode 3830 during the bottle-firing stop are calibrated with sufficient reproducibility (<1%; Uchida et al., 2008). For a fast-profiling CTD observation (typical descent and ascent rates are 1 m s^{-1}), however, the Optode 3830 can develop a substantial disequilibrium owing to the relatively slow response time of the sensor (63% response time requires 19 s at a temperature of 26°C and 57 s at a temperature of 0°C) in a strong vertical gradient of oxygen and temperature. Moreover, the resulting small-scale vertical oxygen profile is considerably smoother than the true data reflect, even when the true oxygen data are somewhat corrected for the slow time response (Fig. 5). In contrast, the Rinko optode has a faster time response than the Optode 3830. The Rinko optode can also measure strong vertical gradients and generate small-scale vertical oxygen profiles in a fast-profiling CTD observation (Fig. 5). Since the sensing foil is slightly modified from that of the prototype optode in order to reduce the time drift of the optode, the pressure compensation coefficient should be reevaluated during development of successor Rinko optodes.

Just recently, Aanderaa Data Instruments AS developed a new model of the oxygen optode (model 4330F). The Optode 4330F contains a fast-response sensing foil (63% response time requires 10 s at a temperature of 26°C and 15 s at a temperature of 0°C). For conventional sensing foils, a black optical isolation layer protects the fluorescent indicator from sunlight and fluorescent particles in the water, but this isolation layer increases the amount of time required for oxygen to equilibrate within the foil. In contrast, the fast-response foil does not have such an isolation layer similar to those

used in the Rinko optode. Although the response time is still slow for a fast-profiling CTD observation, it appears preferable to use the Optode 4330F instead of the Optode 3830.

4. ACKNOWLEDGEMENTS

5. REFERENCES

Atkinson, J. M., F. I. M. Thomas, and N. Larson. 1996. Effects of pressure on oxygen sensors. *J. Atmos. Oceanic Technol.* 13, 1267–1274.

Benson, B. B., and D. Krause, Jr. 1984. The concentration and isotopic fractionation of gases dissolved in freshwater in equilibrium with the atmosphere. *Limnol. Oceanogr.* 29 (3), 620–632.

Bullister, J. L., and G. C. Johnson. 2009. Cruise Report: P18_2007. 99 pp. Available online at: http://cchdo.ucsd.edu/data_access/show_cruise?ExpoCode=33RO20071215.

Clark, L. C., R. Wolf, D. Granger, and Z. Taylor. 1953. Continuous recording of blood oxygen tensions by polarography. *J. Appl. Physiol.* 6, 189-193.

Demas, J. N., B. A. De Graff and P. Coleman. 1999. Oxygen sensors based on luminescence quenching. *Anal. Chem.* 71, 793A–800A.

Edwards, B., D. Murphy, C. Janzen, and N. Larson. 2010. Calibration, response, and hysteresis in deep sea dissolved oxygen measurements. *J. Atmos. Oceanic Technol.* 27, 920-931, doi:10.1175/2009JTECHO693.1.

Dickson, A. G. 1996. Determination of dissolved oxygen in sea water by Winkler titration. In *WOCE operations manual, WHP operations and methods*, WHPO 91-1, WOCE Rep. 68/91, WOCE International Project Office, 13 pp.

García, H. E. and L. I. Gordon. 1992. Oxygen solubility in seawater: Better fitting equations. *Limnol. Oceanogr.* 37 (6), 1307–1312.

Kanwisher, J. 1959. Polarographic oxygen electrode. *Limnol. Oceanogr.* 4(2), 210–217.

Klimant, I., V. Meyer and M. Kühl. 1995. Fiber-optic oxygen microsensors, a new tool in aquatic biology. *Limnol. Oceanogr.* 40 (6), 1159–1165.

Körtzinger, A., J. Schimanski and U. Send. 2005. High quality oxygen measurements from profiling floats: A promising new technique. *J. Atmos. Oceanic Technol.* 22, 302–308.

Millard Jr., R. C. 1994. CTD oxygen calibration procedure. In *WOCE Operations Manual*, *WHP Operations and Methods*, WHPO 91-1, WOCE Int. Project Office, WOCE Report No. 68/91, November 1994, rev. 1.

Murata, A., H. Uchida and K. Sasaki. 2009. R/V Mirai Cruise Report, MR09-01. Available online at : http://www.jamstec.go.jp/cruisedata/mirai/e/MR09-01_leg1.html.

Owens, W. B., and R. C. Millard Jr. 1985. A new algorithm for CTD oxygen calibration. *J. Phys. Oceanogr.* 15, 621-631.

Press, W. H., S. A. Teukolsky, W. T. Vetterling and B. P. Flannery. 1992. *Numerical Recipes in FORTRAN: The Art of Scientific Computing Second Edition*. 963pp., Cambridge University Press, Cambridge.

Sea-Bird Electronics, Inc. 2009. SBE 43 dissolved oxygen (DO) sensor – Hysteresis corrections, Application note no. 64-3, 7 pp.

Swift, J. H., and G. C. Johnson. 2009. US Global Ocean Carbon and Repeat Hydrography Program Cruise I5: Preliminary Cruise Report. 86 pp. Available online at: http://cchdo.ucsd.edu/data_access/show_cruise?ExpoCode=33RR20090320.

Tengberg, A., J. Hovdenes, H. J. Andersson, O. Brocandel, R. Diaz, D. Hebert, T. Arnerich, C. Huber, A. Körtzinger, A. Khripounoff, F. Rey, C. Rönning, J. Schimanski, S. Sommer and A. Stangelmayer. 2006. Evaluation of a lifetime-based optode to measure oxygen in aquatic systems. *Limnol. Oceanogr. Methods* 4, 7–17.

Uchida, H., T. Kawano, I. Kaneko and M. Fukasawa. 2008. In situ calibration of optode-based oxygen sensors. *J. Atmos. Oceanic Technol.* 25, 2271–2281.

Table 1. Sample values of pre-set coefficients for nonlinear parameter estimation for the Optode 3830 and Rinko optode.   The remaining four coefficients (c_1, c_2, d_0, and d_1) are pre-set to zero.

Coefficient	Optode 3830	Rinko
c_0	0.003	0.008
d_2	0.017 [(°)$^{-1}$]	0.2 [V^{-1}] *

----

* For an output range of 0–5 V

Figure 1. Oxygen concentration (μmol L^{-1}) plotted against ratio of phase shift (P_0/P) with regressions (dashed lines). Results from the manufacturer's calibration for a batch of foil (no. 4104) of Optode 3830 are used to create this plot.
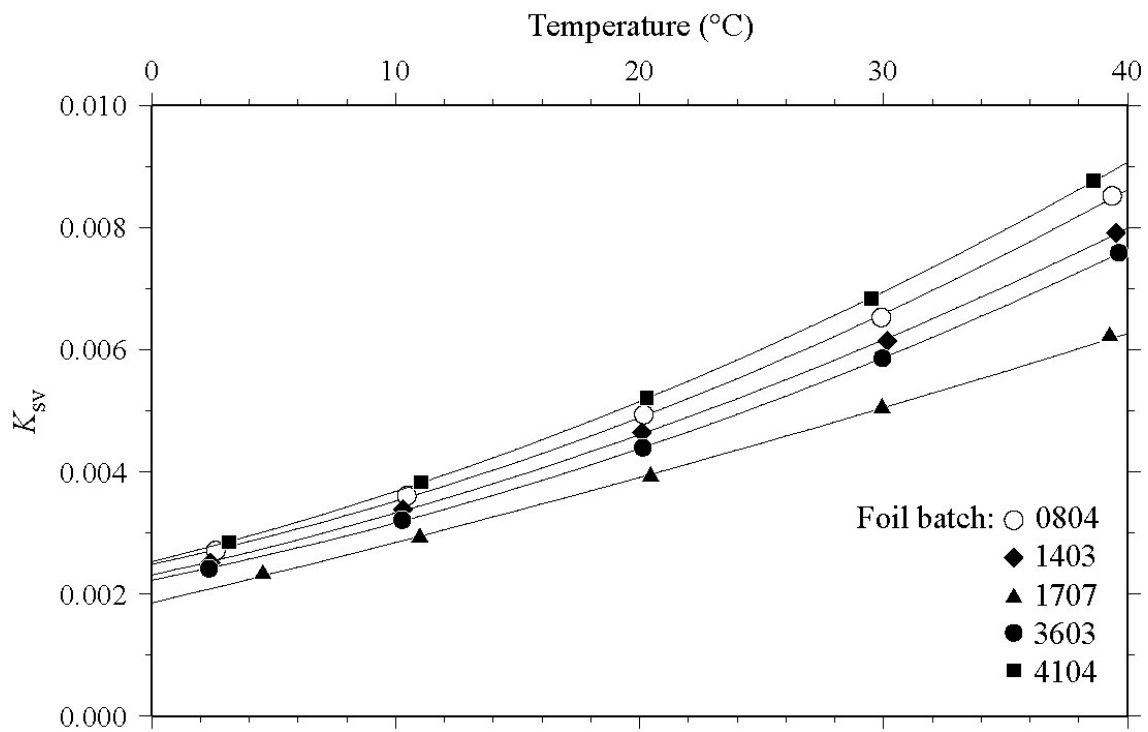
Figure 2. Temperature dependence of the Stern–Volmer constant (K_{sv}) based on results of the manufacturer's calibration for five batches of foil of Optode 3830. K_{sv} as estimated from the slope of the regression line of the Stern–Volmer plot (Fig. 1) with best-fitting second-order polynomial curves (solid lines).
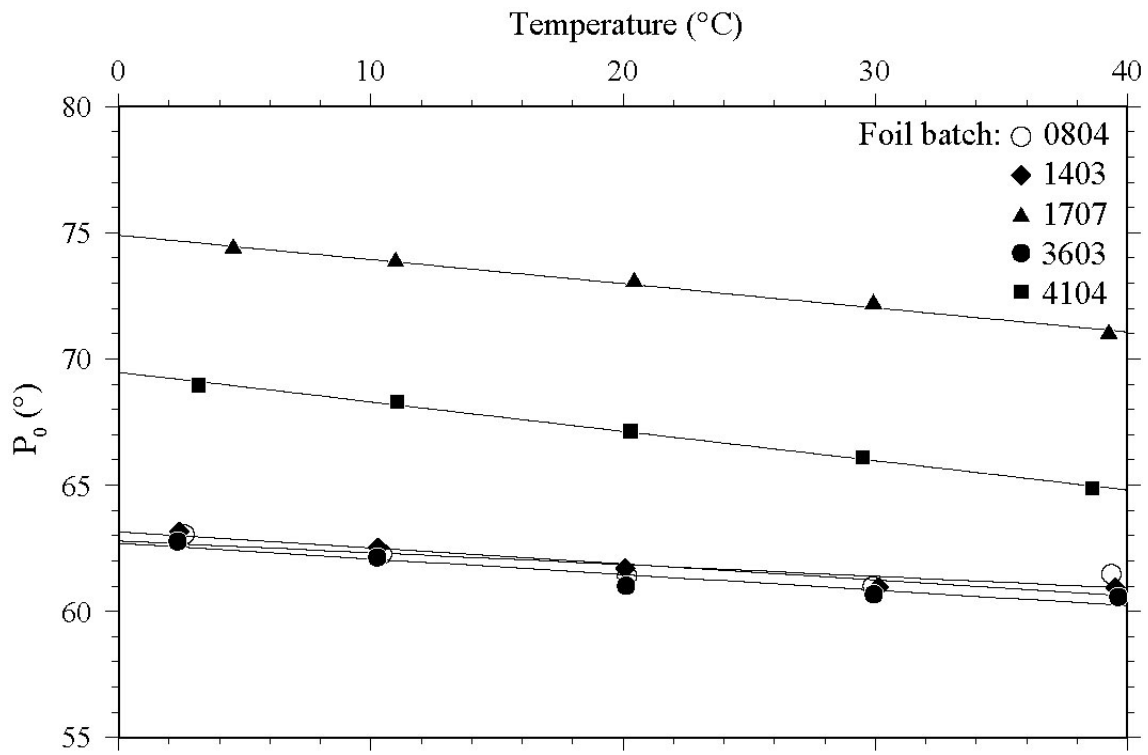
Figure 3. Temperature dependence of the phase shift in the absence of [O₂] based on results of the manufacturer's calibration for five batches of foil of Optode 3830 with regressions (solid lines).
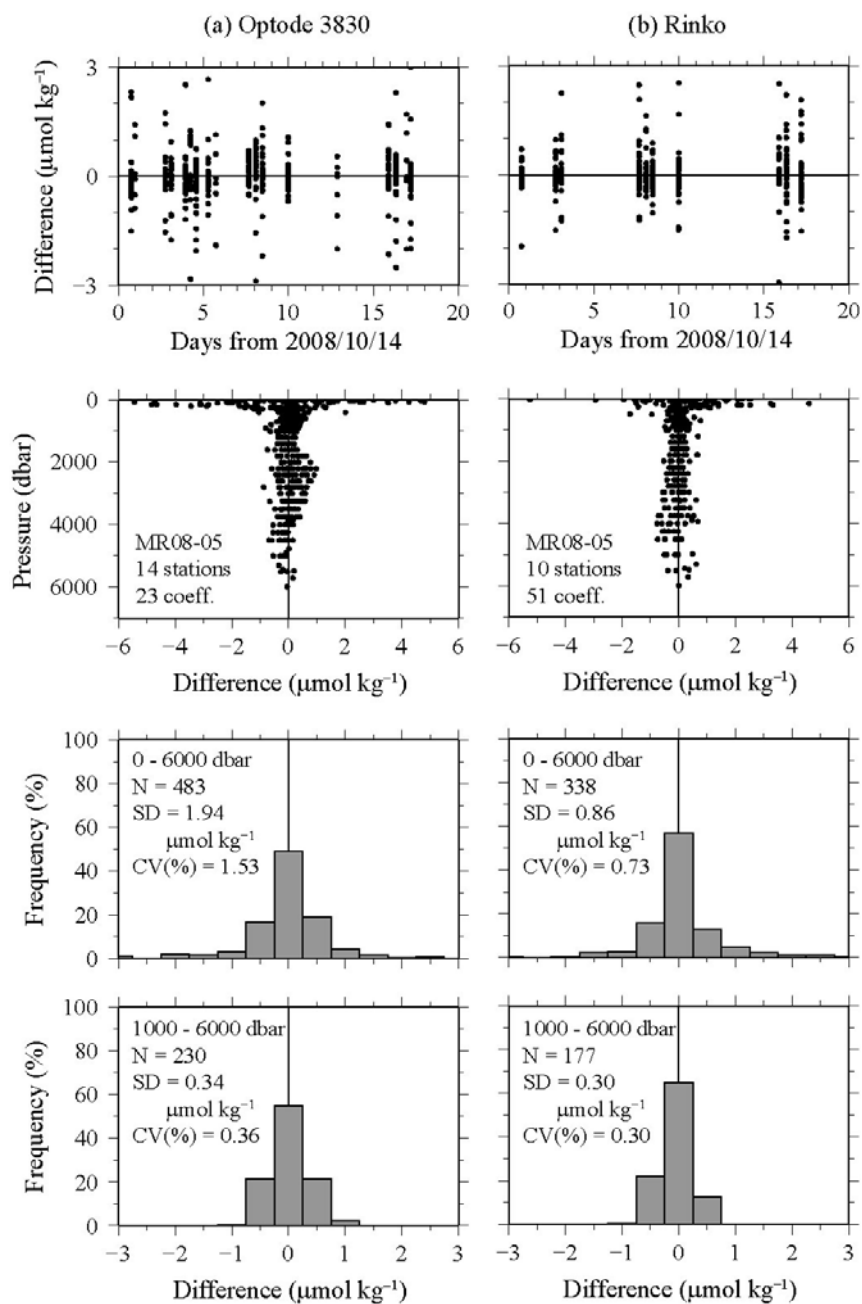
Figure 4. Differences between in situ calibrated oxygen data and Winkler oxygen data for (a) Optode 3830 and (b) a Rinko optode plotted against time (upper panels) and pressure (upper-middle panels). Histograms of the differences are also shown (lower-middle and lower panels for full depth and for pressure ≥ 1000 dbar, respectively). Data were collected in the Bering Sea and the northwest subarctic Pacific Ocean on the R/V *Mirai* cruise MR08-05.
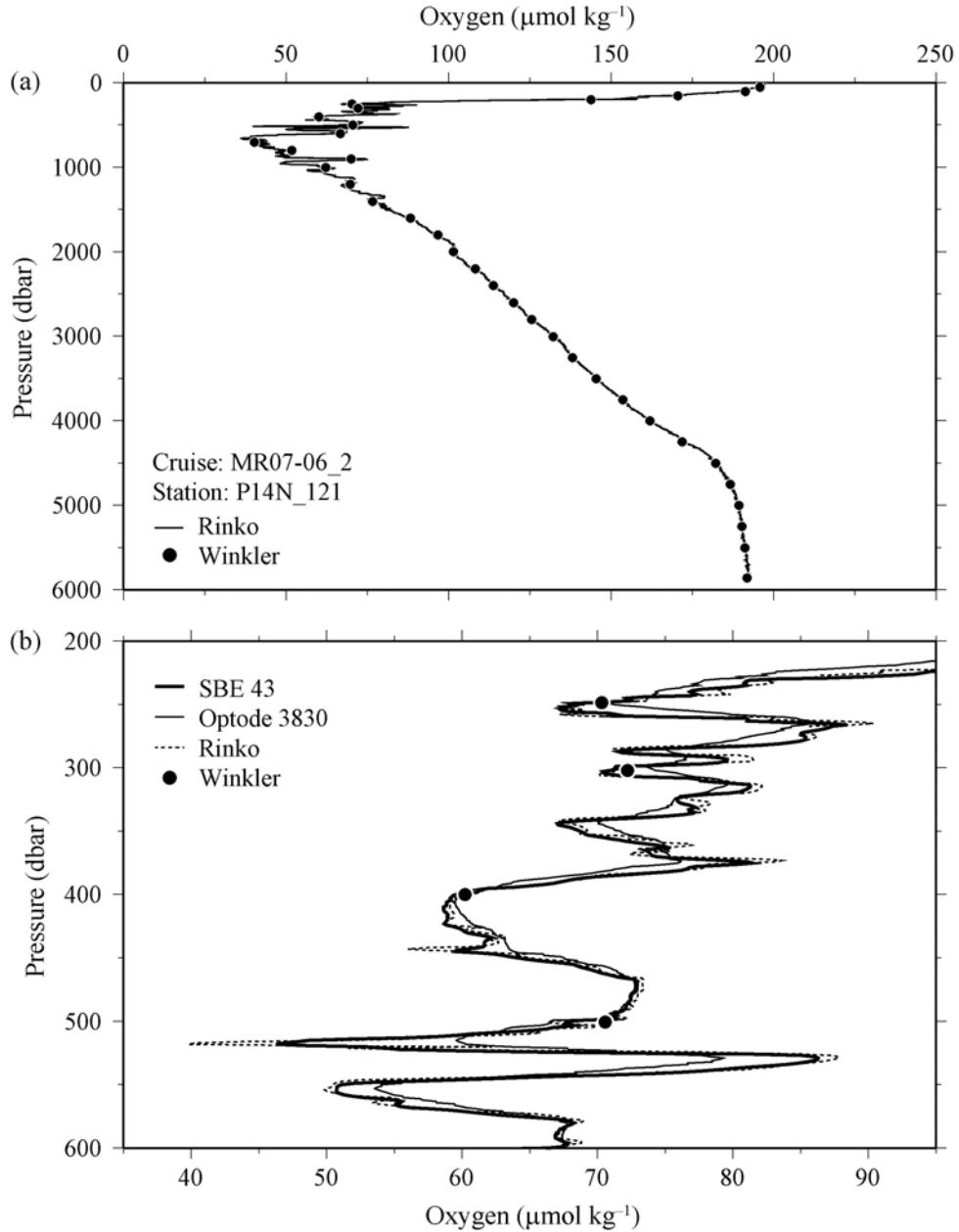
Figure 5. Vertical oxygen profiles obtained with in situ calibrated oxygen sensors (SBE 43, Optode 3830, and Rinko) and Winkler oxygen data from discrete water samples of the R/V *Mirai* cruise MR07-06 leg 2 station P14N_121 (5° 30'N, 179°E).   (b) An enlargement of (a) for depths between 200 and 600 dbar.   The Optode 3830 data are compensated for the temperature-dependent delay due to the slow response time of the sensor (Uchida et al., 2008).